

Orientation dependence of grain-boundary critical current densities in high- T_c bicrystals

T. Amrein* and L. Schultz†

SIEMENS AG, Research Laboratories, BT MR 1, P.O. Box 3220, D-91050 Erlangen, Germany

B. Kabius and K. Urban

IFF/IMF, Forschungszentrum Jülich GmbH, D-52425 Jülich, Germany

(Received 14 December 1994)

The critical current density across grain boundaries of twinned thin-film $\text{Bi}_2\text{Sr}_2\text{CaCu}_2\text{O}_{8+x}$ bicrystals has been measured as a function of the tilt angle Θ . For $\Theta=0^\circ$ to 45° , the ratio of intergrain to intragrain critical current density decreases exponentially with increasing tilt angle. Surprisingly, this orientation dependence is very similar to that observed for $\text{YBa}_2\text{Cu}_3\text{O}_7$ bicrystals. Microstructural investigations of plan view samples show a wavy grain boundary of the superconductor with a roughness of 100 nm to $1\ \mu\text{m}$ which does not originate from the roughness of the substrate grain boundary (1–3 nm) but is caused by an island-plus-layer growth of twin domains. In general, one of the adjacent grains has a low-indexed habit plane at the boundary.

Whereas the critical current density, j_c , of thin films of high- T_c superconductors (HTS's) is already high enough for numerous applications, polycrystalline materials, which are required for making wires or tapes, are characterized by rather low current densities. A variety of effects is responsible for the low j_c of polycrystalline HTS's.¹ However, j_c in polycrystals is lowered by voids, cracks, and second phases. Furthermore, in nonoriented grains, the current has to flow along the c direction, which has a low j_c . Finally, grain boundaries (GB's) reduce j_c , in contrast to certain low- T_c superconductors, in which GB's enhance j_c by acting as pinning sites. The reason is that in HTS's the extremely short coherence length of about $\xi_{ab}=1$ nm causes poor coupling of the superconducting order parameter across grain boundaries. Therefore, HTS-GB's act as weak links. This behavior has been utilized to fabricate Josephson junctions of high quality by using thin film bicrystals of either $\text{YBa}_2\text{Cu}_3\text{O}_7$ (YBCO) or $\text{Bi}_2\text{Sr}_2\text{CaCu}_2\text{O}_{8+x}$ (BSCCO).^{2,3} Unfortunately, the short coherence length is responsible for the sensitivity of the electrical properties on small defects, too. Thus, it is difficult to correlate the macroscopic properties to microstructural features and vice versa.

By measuring the superconducting transport properties of individual grain boundaries and their adjacent grains in YBCO thin film bicrystals, Dimos *et al.* demonstrated that the critical current across a GB, j_c^{gb} , is quite sensitive to the misorientation angle Θ .⁴ Since then, emphasis was put on the investigation of transport properties of GB's but the effort was mainly restricted to YBCO due to the high quality of thin films.^{5,6}

In the following, some properties of single, artificial GB's in high-quality thin film bicrystals of BSCCO will be presented. The measurement of the critical current density as a function of the misorientation angle in conjunction with high-resolution transmission electron microscopy gives new information on the superconducting transport properties of GB's. Additionally, the film growth across the substrate GB will be presented schematically.

BSCCO films, about 200 to 400 nm thick, were deposited by excimer laser ablation on commercially available SrTiO_3

bicrystals.³ Bicrystalline substrates with various tilt angles (10° , 24° , 36.8° , and 45°) were used. For both grains, the normal of the substrate is almost parallel to the [100] direction, which in turn is the rotational axis of the tilt GB. BSCCO grain boundary junctions (GBJ's) were created by patterning a microbridge, typically a few micrometers in width and length, across the GB of the bicrystalline BSCCO film. The films were either dry etched by Ar^+ -ion beam milling or wet etched with EDTA (ethylenediaminetetraacetic acid) in water. The GBJ's could be manufactured with a yield of 85%. Both grains of each GBJ are c axis oriented and show a smooth surface. Critical temperatures of the thin films, $T_c(R=0)$, vary between 87 and 91 K. The critical current density of the grains, j_c^g , amounts to $2\text{--}5 \times 10^5$ A/cm² at 77 K.

The transport properties of about 250 BSCCO GBJ's have been studied extensively by measuring the current (I)–voltage (V) characteristics at 4.2 and 77 K using a common four-point technique. GB's with a tilt angle $\Theta > 10^\circ$ behave like Josephson junctions. Their j_c^{gb} 's are highly sensitive to magnetic fields. For $\Theta > 24^\circ$, a resistively shunted junction (RSJ)-like behavior could be observed.³ All of them are noise rounded at 77 K due to the thermally activated phase slippage.⁷ In view of that, the critical current, I_c , has been determined by the intersection of the tangent $(dI/dV)_{\min}$ with the current axis. In Fig. 1(a) and 1(b) the $j_c^{gb}(\Theta)$ dependencies of a, b -tilt BSCCO at 4.2 and 77 K are compared with data obtained for YBCO GBJ's.⁸ Each data point represents the average value of all measured GBJ's (10 to 22) on one HTS chip. The error bars give the standard deviations. The solid lines are obtained from least-square fits. Whereas the observed $j_c^{gb}(\Theta)$ dependency is similar for bicrystalline BSCCO and YBCO GBJ's, the absolute magnitude of $j_c^{gb}(\Theta)$ is about ten times smaller for BSCCO GBJ's. This correlates with the fact that the intragrain critical current density, $j_c^g \approx j_c^{gb}(0^\circ)$, in YBCO samples is about one order of magnitude larger than that in BSCCO samples. The ratio $j_c^{gb}(\Theta)/j_c^g$ as a function of the tilt angle Θ is given in

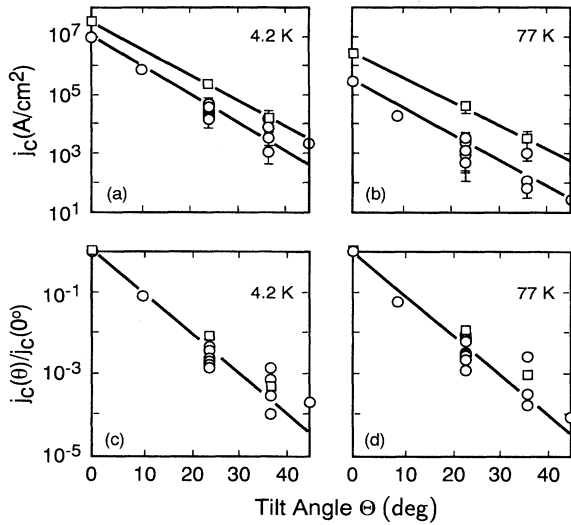


FIG. 1. (a) and (b) Average value of the grain-boundary critical current density of a chip as a function of tilt angle Θ . (c) and (d) Ratio of the intergrain and the intragrain critical current density as a function of tilt angle Θ . [\circ : $\text{Bi}_2\text{Sr}_2\text{CaCu}_2\text{O}_{8+x}$, \square : $\text{YBa}_2\text{Cu}_3\text{O}_7$ (Ref. 7)].

Fig. 1(c) and 1(d). Both superconductors show an almost identical exponential decrease:

$$\frac{j_c^{gb}(\Theta)}{j_c^g} = \exp(-a\Theta) \quad \text{with } a \approx 0.2. \quad (1)$$

In addition, the exponential factor a does not depend on the temperature. Relation (1) agrees very well with data reported in the literature for YBCO GBJ's on bicrystalline substrates,⁹ e.g. MgO ,¹⁰ silicon,¹¹ SrTiO_3 ,^{6,12} or Y-ZrO_2 .¹² Thus, the factor a does not depend on the chosen substrate, either. We want to emphasize that a saturation of $j_c^{gb}(\Theta > 20^\circ)/j_c^g$ to a value of about 0.02 as published in Ref. 4 could neither be corroborated in our work nor in recent investigations on high-quality GBJ's.^{6,10-12}

The microstructure of the GB's with $\Theta = 24^\circ$ and 36.8° has been examined using high-resolution electron microscopy (HREM). Figure 2(a) shows a bright field image of a 36.8° GB in BSCCO. The GB, marked F , runs along the domain boundaries of the 90° rotation twin structure¹³ (\rightarrow : b direction of the BSCCO compound). The roughness of the GB is equivalent to the size of the twin domains and varies between 100 and 300 nm. Therefore, the roughness of the film GB is not determined by the roughness of the substrate GB (S), which is in the order of 1 nm (see Fig. 2 in Ref. 14), but rather by the growth of twin domains. In general, one of the adjacent grains has a low-indexed habit plane at the GB, especially (100) and (010) habit planes exist quite often. Figure 2(b) shows a lattice fringe image of a 36.8° GB. The change from an $x/(100)$ (top) to an $(100)/x$ GB (bottom) is obvious in this micrograph, where x represents a high-indexed habit plane which is only determined by the misorientation angle and therefore is a function of Θ . The density of crystallographic defects near the GB (< 10 nm) is not larger than within the grains. It should be noted that the

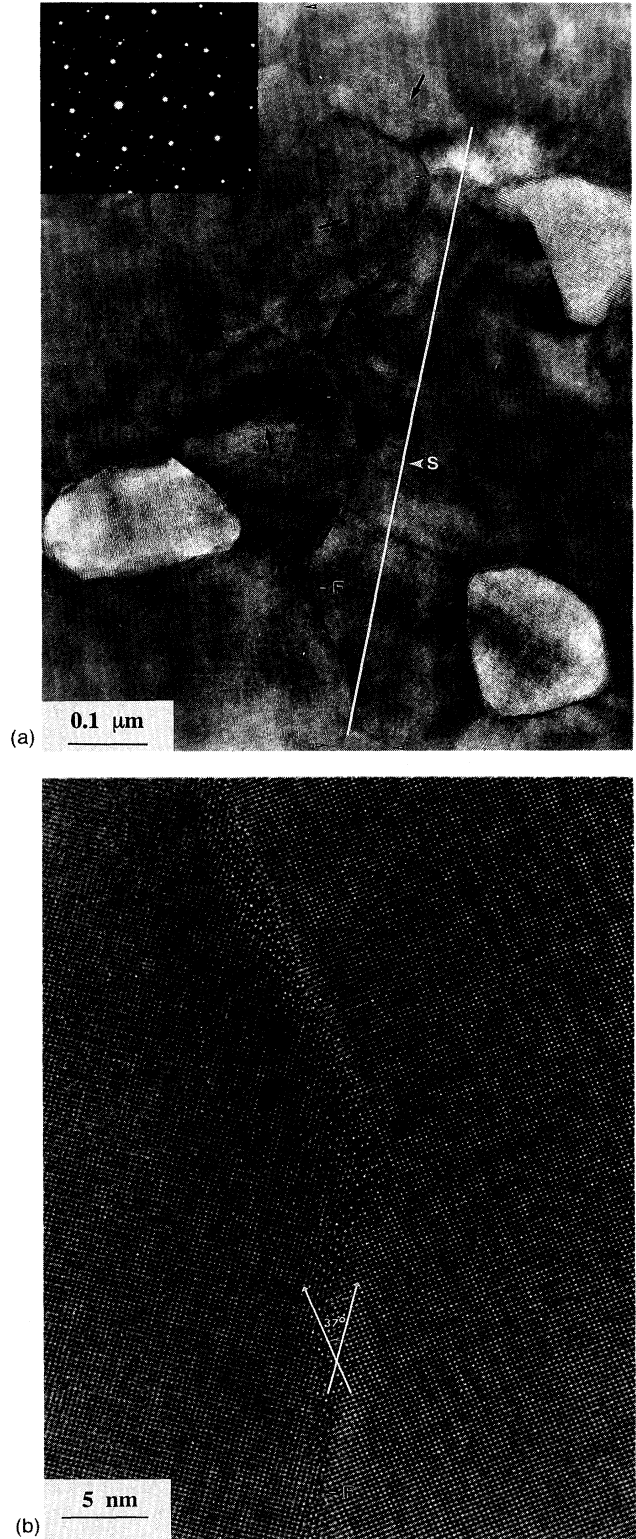


FIG. 2. (a) Diffraction contrast image and (b) lattice fringe image of a 36.8° grain boundary in $\text{Bi}_2\text{Sr}_2\text{CaCu}_2\text{O}_{8+x}$. The inset in (a) shows the selected area electron diffraction pattern. F : grain boundary of thin film, S : grain boundary of substrate, \rightarrow : b direction of the $\text{Bi}_2\text{Sr}_2\text{CaCu}_2\text{O}_{8+x}$ compound (Ref. 12).

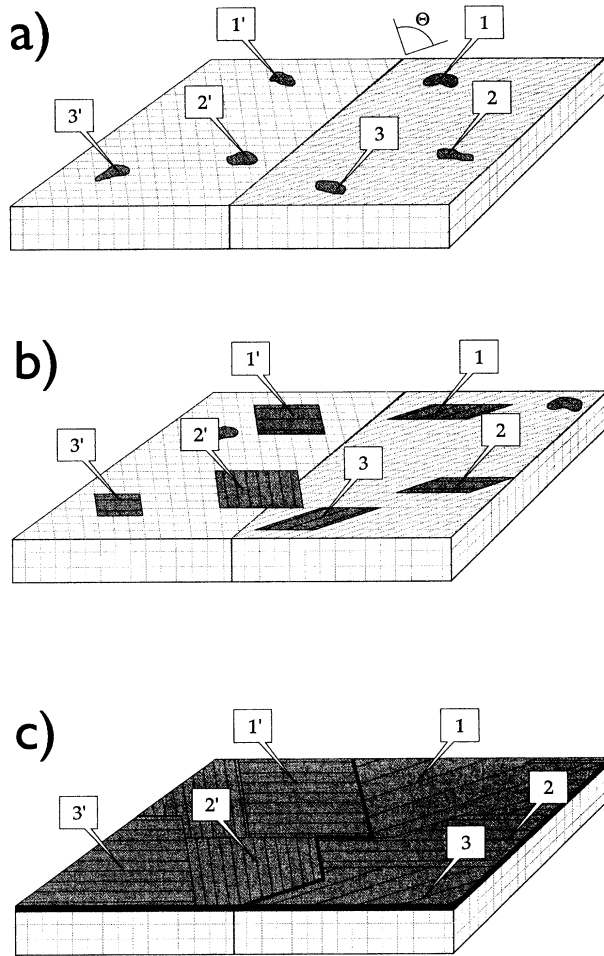


FIG. 3. Schematic representation of growth stages involved in initial film growth across the grain boundary of bicrystalline substrates. The thin film material is shown as dark areas, the substrate as light areas. The cubic cells visualize the crystalline structure of the substrate. The lateral length of one cell is of the order of 50 nm.

microstructure of GB's in YBCO thin films shows similar characteristics. A detailed description is given in Ref. 14).

The observed wavy form of HTS GB's is caused by the film growth during deposition. Since an island-plus-layer growth was observed in our prior study of a series of ultrathin BSCCO films,¹⁵ a model of the film growth across the substrate GB is near at hand: Small circular nuclei begin to grow during the initial stage of film deposition. Their distribution over the substrate surface is more or less statistically [Fig. 3(a)]. Later, the nuclei expand forming plateaus. Further growth leads to rectangular islands with leading edges along [100] and [010] directions of the film [Fig. 3(b)]. Some islands start to grow across the grain boundary of the substrate preserving their original epitaxial relationship due to the weak bonding between film and substrate [2' in Fig. 3(b)]. The islands coalesce into thicker films (>25 nm) and form the wavy GB within the superconducting film [Fig. 3(c)]. In addition to this simplified model, the z-shaped GB is smoothed to an s-shaped GB [Fig. 2(b)]. The microstruc-

ture of sputtered ultrathin films of YBCO on MgO had been studied by Streiffer *et al.*¹⁶ using HREM. Here, only very thin films with a thickness <12 nm consisted of interconnected islands, whereas thicker films showed a complete coverage of the surface. If we assume a similar growth mechanism for YBCO films on SrTiO₃ then the significantly smaller roughness of YBCO GB's [10 to 200 nm (Ref. 14)] in comparison to BSCCO GB's (100 nm to 1 μm) can be explained by the different film thickness required for complete coverage.

In conclusion, the microstructure of the HTS GB's is determined by the lateral growth characteristics of each compound and the coalescence of islands during the initial stage of deposition. It is expected that the meander structure of the GB causes inhomogeneities of j_c^{gb} on a scale of a few tens of nanometers or less. This result is important for device applications considering e.g., magnetic-field dependence or flux noise of Josephson junctions.³ Frequent occurrences of the (100) $x(\Theta)$ or (010) $x'(\Theta)$ GB lets us assume that their atomic structure and fractional length, $f(\Theta)$, determine the transport properties on a macroscopic scale, especially the angular dependence of j_c^{gb} , since both depend on Θ . Considering the model of Jagannadham and Narayan,¹⁷ the ratio of intergrain to intragrain critical current density is given by

$$\frac{j_c^{gb}(\Theta)}{j_c^g} = \epsilon_{gb}^2(\Theta) f_T^2(\Theta) T_j. \quad (2)$$

Here, $\epsilon_{gb} = \Delta_{gb}(T, \Theta) / \Delta_0(T)$ represents the depression of the order parameter at the GB. In Ref. 17, f_T is the fractional length of the coalesced region along the boundary available for the tunneling of Cooper pairs. We assume that f_T is almost equal to $f(\Theta)$. The transmission coefficient of the GB, $T_j = \exp[-t(\Theta) / \xi_0]$, depends on the width of the GB, $t(\Theta)$, and the coherence length ξ_0 . Since ϵ_{gb} can be used as a fit parameter of the Ambegaokar-Baratoff formula by fitting the experimental temperature dependence of $j_c^{gb}(\Theta) / j_c^g$, we know that ϵ_{gb} reveals a weak Θ dependence: ϵ_{gb} decreases from 0.28 for $\Theta = 10^\circ$ to 0.1 for $\Theta = 45^\circ$. Thus, the exponential decrease of j_c^{gb} with increasing Θ , as described by Eq. (1), is caused by the exponential decrease of the transmission coefficient. (Note that the width of the boundary, t , in units of ξ_0 has a weak dependence of Θ if $\Theta \geq 10^\circ$.¹⁷) Last but not least, we want to emphasize that substrate lattices with low coincidence values Σ , e.g., $\Sigma(\Theta = 36.8^\circ) = 5$, are of no particular relevance with respect to transport properties or microstructure. This is a direct consequence of the film growth described above.

The result that two of the high- T_c cuprates show the same sensitive angular dependence of j_c^{gb} has important consequences. For example, polycrystalline YBCO samples, such as wires, fibers or tapes, have to carry ten times the critical current densities of BSCCO samples of the same morphology. Nevertheless, the high j_c 's in silver sheathed BSCCO wires are caused by the preparation of a high-textured microstructure, wherein the c axis of the platelet-shaped grains are nearly parallel (see, e.g., "brick-wall model" in Ref. 1). Furthermore, the grains are aligned biaxially to within a few degrees. In contrast, polycrystalline YBCO samples are mostly low textured and less aligned which results in low j_c 's.

- *Present address: Philips Research Laboratories, LB, Weißhausstraße 2, D-52066 Aachen, Germany.
- †Present address: Institut für Metallische Werkstoffe, IFW Dresden, Helmholtzstraße 20, D-01069 Dresden, Germany.
- ¹J. Mannhart and C. C. Tsuei, *Z. Phys. B* **77**, 53 (1989).
- ²P. Chaudhari, J. Mannhart, D. Dimos, D. D. Tsuei, J. Chi, M. M. Oprysko, and M. Scheuermann, *Phys. Rev. Lett.* **60**, 1653 (1988).
- ³T. Amrein, M. Seitz, D. Uhl, L. Schultz, and K. Urban, *Appl. Phys. Lett.* **63**, 1978 (1993).
- ⁴D. Dimos, P. Chaudhari, J. Mannhart, and F. K. LeGoues, *Phys. Rev. Lett.* **61**, 219 (1988).
- ⁵D. Dimos, P. Chaudhari, and J. Mannhart, *Phys. Rev. B* **41**, 4038 (1990).
- ⁶R. Gross and B. Mayer, *Physica C* **180**, 235 (1991).
- ⁷R. Gross, P. Chaudhari, D. Dimos, A. Gupta, and G. Koren, *Phys. Rev. Lett.* **64**, 228 (1990).
- ⁸M. Seitz (private communication).
- ⁹Tl-Ba-Ca-Cu-O GB's on SrTiO₃ bicrystal substrates show a slower decrease ($a < 0.2$). From E. Sarnelli, P. Chaudhari, W. Y. Lee, and E. Esposito, *Appl. Phys. Lett.* **65**, 362 (1994).
- ¹⁰H. B. Lu, T. W. Huang, J. J. Wang, J. Lin, S. L. Tu, S. J. Yang, and S. E. Hus, *IEEE Trans. Appl. Supercond.* **3**, 2325 (1993).
- ¹¹J. Chen, T. Yamashita, H. Suzuki, H. Myoren, K. Nakajima, and Y. Osaka, *IEEE Trans. Appl. Supercond.* **3**, 2333 (1993).
- ¹²P. Å. Nilsson, Z. G. Ivanov, H. K. Olsson, D. Winkler, T. Claeson, E. A. Stepanov, and A. Ya. Tsalenchuk, *J. Appl. Phys.* **75**, 7972 (1994).
- ¹³The twin structure results from the incommensurable superstructure along the b direction of the BSCCO compound ($b^* \approx 4.8b \approx 26.3 \text{ \AA}$).
- ¹⁴B. Kabius, J. W. Seo, T. Amrein, M. Siegel, K. Urban, and L. Schultz, *Physica C* **231**, 123 (1994).
- ¹⁵T. Amrein, B. Kabius, J. Burger, G. Saemann-Ischenko, L. Schultz, and K. Urban, *J. Alloys Compounds* **195**, 129 (1993).
- ¹⁶S. K. Streiffer, B. M. Lairson, C. B. Eom, B. M. Clemens, J. C. Braverman, and T. H. Geballe, *Phys. Rev. B* **43**, 13 007 (1991).
- ¹⁷K. Jagannadham and J. Narayan, *Mater. Sci. Eng.* **14**, 214 (1992).

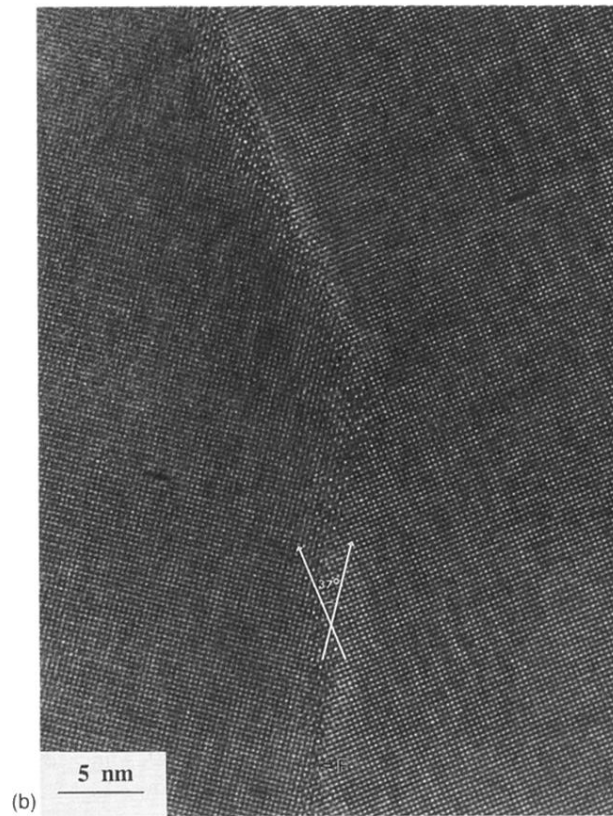
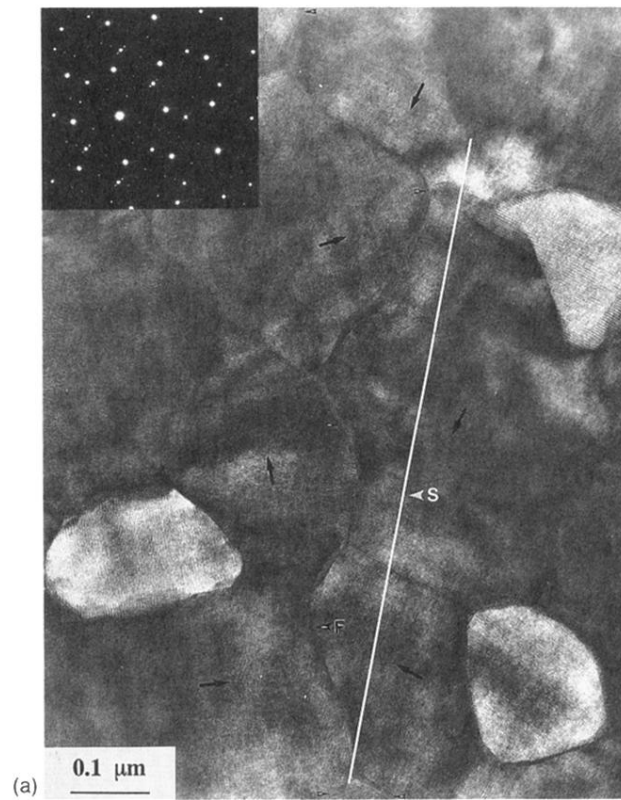


FIG. 2. (a) Diffraction contrast image and (b) lattice fringe image of a 36.8° grain boundary in $\text{Bi}_2\text{Sr}_2\text{CaCu}_2\text{O}_{8+x}$. The inset in (a) shows the selected area electron diffraction pattern. *F*: grain boundary of thin film, *S*: grain boundary of substrate, \rightarrow : *b* direction of the $\text{Bi}_2\text{Sr}_2\text{CaCu}_2\text{O}_{8+x}$ compound (Ref. 12).

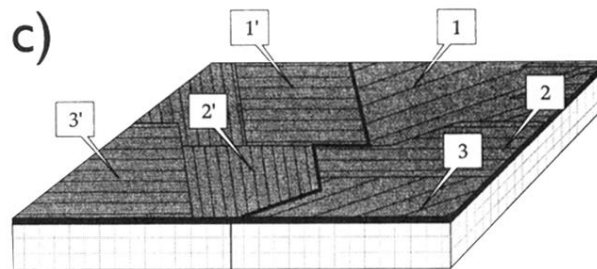
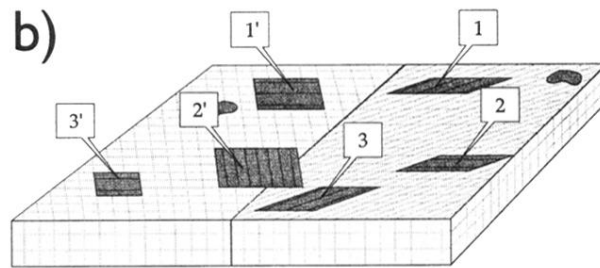
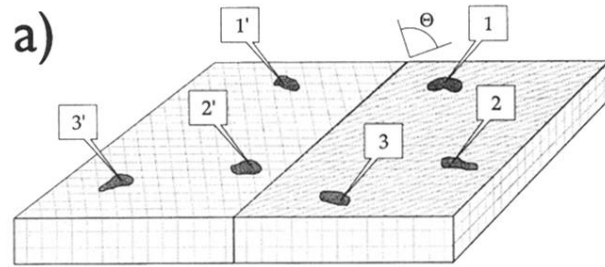


FIG. 3. Schematic representation of growth stages involved in initial film growth across the grain boundary of bicrystalline substrates. The thin film material is shown as dark areas, the substrate as light areas. The cubic cells visualize the crystalline structure of the substrate. The lateral length of one cell is of the order of 50 nm.